

# **Characteristics and Applications of the Injection-Locked Semiconductor Lasers**

•

# **Characteristics and Applications of the Injection-Locked Semiconductor Lasers**

1999

12

▪



# Index

Table Index-----	iii
Figure Index-----	iv
-----	vi
I. Introduction-----	1
II. OIL Characteristics-----	4
A. Locking Range .....	4
B. Transient / Spectral Response .....	5
III. OIL Modulation Response-----	12
A. Small-Signal Modulation.....	12
B. Large-Signal Modulation.....	20
C. Rf-Modulation Properties .....	21
IV. OIL Applications-----	25
A. Fiber-Optic Transmission.....	25
B. Optical Analog Transmission.....	33
C. Optical Generation of mm- wave signals .....	34

V. Summary-----	45
VI. References-----	47
Abstract-----	50

## Table Index

Table I. Simulation parameter values of the laser -----7

## Figure Index

Fig. 1. Basic OIL configuration-----	3
Fig. 2. Characteristics of locking regimes-----	8
Fig. 3. Transient solution of the lasers at different locking conditions----- -----	9
Fig. 4. Spectral responses of the laser at the different locking conditions-- -----	11
Fig. 5. Dependence of the amplitude modulation response on the injected power and frequency offset-----	14
Fig. 6. OIL modulation bandwidth normalized by the intrinsic modulation bandwidth-----	15
Fig. 7. Dependence of frequency chirp on the injected power and the frequency offset-----	16
Fig. 8. The transient solutions of the rate equations-----	19
Fig. 9. Simulation block diagram for the laser under rf-modulation----- -----	22
Fig. 10. The frequency response of max. freq. deviations -----	23
Fig. 11. Optical spectra of the field of lasers with varying $I_{p-p}$ - ----- -----	24
Fig. 12. Schematic of numerical simulation -----	28
Fig. 13. BER curves for the free-running and injection-locked lasers----- -----	29

Fig. 14. Dependence of the receiver sensitivity on the fiber-optic length--	30
Fig. 15. Dependence of the receiver sensitivity on the extinction ratio----	31
Fig. 16. Dependence of receiver sensitivity on transmission speed-----	32
Fig. 17. Basic block diagram for the experiment-----	35
Fig. 18. Simulated spectral amplitudes-----	36
Fig. 19. Simulated modulation frequency responses-----	37
Fig. 20. Measured spectral amplitudes-----	38
Fig. 21. Measured rf-spectra of free-running and injection-locked lasers--	39
Fig. 22. Block diagrams for the typical and the proposed OIL technique for $\mu$ - / mm- wave generation-----	42
Fig. 23. Calculated power spectra of the injection-locked lasers in the unstable-locking regime-----	43
Fig. 24. The sideband separation as function of R along the boundary in Fig. 2-----	44



# Injection Locking

Injection locking , ,  
 . , rate-equations  
가 . Locking  
 . locking locking  
 .  
 / optical injection locking (OIL)  
 , frequency chirp  
 . , FM frequency  
chirp multi-tone rf-  
 . , two-tone rf- injection locking  
 .  
 bit error rate , OIL  
 . 가 ,  
 , extinction ratio,  
 . OIL  
 .  
 . OIL  
 .  
 OIL

OIL  
 chirp  
 inter-modulation product analog  
 OIL  
 , 가  
 , strong optical injection  
 mm-wave  
 Unstable-locking  
 sideband sideband slave laser 가  
 , rf-source 가  $\mu$ - / mm- wave  
 가  
 .

---

: Injection locking, , Chirp ,  
 , mm-wave

# I. Introduction

With the information and communication networks in common, the rapid increase in the demand of information requires the development of the ultra-fast communication links to cope with the large capacity of information in the ultra-fast speed. Technologically advanced countries, such as USA, Japan, and EU, have been investigating implementation of ultra-fast optical communication links, and demonstrating large capacity communication links using the wavelength-division multiplexing (WDM) method. The high-speed laser diode (LD) plays a key role in the ultra-fast optical communication area, since the LD modulation speed mainly dominates the information transmission speed of the optical communication links. Therefore, there have been many researches for the increase of the LD modulation speed.

In the optical communication, the digital modulation, combination of '0' and '1', is widely used. Its simple and compact implementation is the direct modulation method. Recently, it is reported under direct modulation that a GaAs LD has its modulation bandwidth over 40 GHz [1] and a LD has the modulation bandwidth of 30 GHz in the range of 1.5  $\mu\text{m}$  wavelength as well [2]. However, the most ordinary commercial LD has the limited modulation bandwidth. In addition, the LD direct modulation produces the frequency chirp, broadens the optical pulse due to the fiber dispersion combined with the frequency chirp, and results in the degradation of long-haul fiber-optic transmission system. As one method of overcoming these limited modulation bandwidth and chirp properties, the optical injection locking (OIL) technique has been investigated.

As seen in Fig. 1, the injection locking method consists of two LD's, where the light from one LD (master laser, ML) is injected into the other LD (slave laser, SL). It is possible to reduce the noise, suppress the mode hopping, and enhance the coherency. OIL reduces the frequency chirp, and enhances the modulation bandwidth three or four times more than the intrinsic modulation

bandwidth [3-6], when the laser with injection locking is directly modulated. In addition, the enhanced LD properties by OIL can contribute to the fiber-optic transmission performance [7-8], as well as can be utilized in the optical repeater of WLL system, CATV, satellite communication, and optical mm-wave generation [9-12].

In this paper, characteristics and applications of the semiconductor lasers under optical injection are investigated. First, Section II deals with locking properties, including the locking range, and transient / spectral responses under different locking conditions. From the steady-state analysis, the locking conditions are classified into three regimes – unlocking, unstable locking, and stable locking. The transient and spectral responses at each regime are distinctive. Second, Section III shows the modulation response of the laser with injection locking under direct modulation. In this section, the relation of modulation bandwidth and frequency chirp with the optical injection is discussed based on the small- / large- signal analyses. Moreover, it is found that the laser rf-modulation response is deeply related with the frequency chirp as well as the optical power. Finally, Section IV deals with the influence of the enhanced LD characteristics by OIL in the applications, including the fiber-optic transmission, optical analog transmission, and optical generation of mm-wave signals.

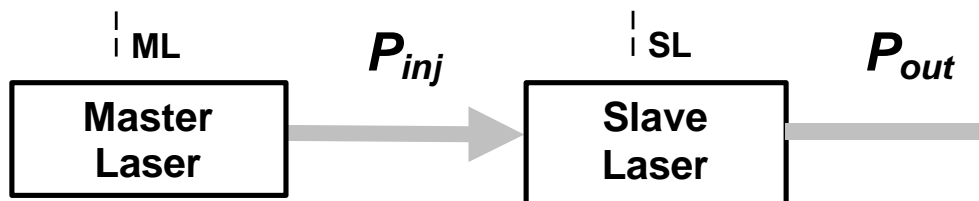


Figure 1. Basic OIL configuration, where the CW light from ML is injected into SL. When SL is perfectly locked to ML, the SL lasing frequency,  $f_{SL}$ , shifts itself to the ML lasing frequency,  $f_{ML}$ .

## II. OIL Characteristics

### A. Locking Range

OIL configuration is made up of a master laser (ML) and a slave laser (SL) as shown in Fig. 1, where CW light from ML is injected into SL. Two lasers have a frequency offset of  $\Delta f$ , where  $\Delta f$  is defined as  $f_{ML} - f_{SL}$ . The polarization problem between ML and SL is not taken into account for simplicity, but the polarization controller should be placed between them for the coupling efficiency in the experiment. Assuming DFB lasers with negligible sidemodes are used for both ML and SL, the SL under the influence of external light injection can be described by the following single-mode rate-equations [13],

$$\frac{dP}{dt} = \left[ \frac{\Gamma g_0}{1 + eP} (N - n_t) - \frac{1}{t_p} \right] P + \frac{\Gamma b}{t_n} N + 2K_C \sqrt{P_{in} P} \cos(\Phi_{ML} - \Phi) \quad (1)$$

$$\frac{d\Phi}{dt} = -2\mathbf{p}\Delta f + \frac{1}{2} \mathbf{a} \left[ \Gamma g_0 (N - n_t) - \frac{1}{t_p} \right] + K_C \sqrt{\frac{P_{in}}{P}} \sin(\Phi_{ML} - \Phi) \quad (2)$$

$$\frac{dN}{dt} = \frac{I}{qV_a} - \frac{g_0}{1 + eP} (N - n_t) P - \frac{N}{t_n} \quad (3)$$

In the above equations,  $P_{in}$  and  $\Phi_{ML}$  represent the density and the phase of the injected photons and  $K_C (= \mathbf{u}_g/2L_a)$  the coupling rate between ML and SL. Other parameters have the usual meanings. The numerical values for the parameters are obtained from [14] and listed in Table. 1.

From the steady-state analysis of the rate-equations, Fig. 2 shows locking regions from unlocking regions as function of  $\Delta f$  and  $R$ . Here, injection power ratio  $R$  is defined as  $P_{inj} / P_{out}$ , where  $P_{inj}$  is the injected optical power just outside the SL facet and  $P_{out}$  is SL output power. For the results shown in Fig. 2, SL output power is fixed at 2 mW. If the gain suppression and the spontaneous emission terms are ignored, the range of  $\Delta f$  that allows locking can be determined as [15],

$$|\Delta f (= f_{ML} - f_{SL})| \leq \frac{K_C}{2\pi} \sqrt{\frac{P_{in}}{P} (1 + \alpha^2)}. \quad (4)$$

This locking range can be further classified into two distinctive regimes: stable-locking and unstable-locking. In the stable-locking regime, the output power converges to a steady-state value when a small perturbation is introduced. In the unstable locking regime, however, the power does not converge to the steady-state value but experiences a self-sustained oscillation or even chaos when a small perturbation is introduced [15]. Such an oscillation and chaos produce multiple sidebands in the output optical spectra. The range for the stable-locking regime can be determined by the s-domain stability analysis of the linearized OIL rate-equations above. The asymmetry of the stable-locking regime is dependent on  $R$ . The center of the stable-locking bandwidth is shifted toward the longer wavelength of SL's lasing wavelength with increasing  $R$ .

## B. Transient / Spectral Response

The SL transient responses under different locking conditions found in Fig. 2 can be solved by the fourth order Runge-Kutta integration of OIL rate-equations, Eq. 1~3. The applying current is abruptly increased from its initial value,  $1.01 \times I_{th}$ , to the final value,  $1.5 \times I_{th}$  when time = 5 ns, here. The laser spectra can be obtained from the fast-Fourier transformation of the SL output power at the steady-state solution of the transient response. The calculated spectra are normalized with SL's peak spectral peak value under no optical injection. In the calculations, noises are not taken into account. The transient and spectral responses are remarkably different depending on the locking conditions as seen in Fig. 3 and 4.

In the unlocking region (Fig. 2-①, -②), either the unlocked power shows up dominantly (Fig. 3-① and Fig. 4-①), or both SL and ML modes as well as four-wave mixing conjugates appear (Fig. 3-② and Fig. 4-②), depending on the

injected power and frequency difference. In the stable-locking region (Fig. 2-③), only the ML mode shows up (Fig. 3-③ and 4-③). Here, SL is locked to ML and has power spectrum only at  $f_{ML}$ . In the unstable-locking region (Fig. 2- ④ and - ⑤), the SL produces chaos (Fig. 3- ④ and Fig. 4-④) and a self-sustained oscillation (Fig. 3- ⑤ and Fig. 4-⑤). The spectrum of chaos is densely spread. It is found that chaos occurs when  $R$  is less than about  $-14$  dB within the unstable locking region, as indicated by shades in Fig. 2. The chaos outside the locking regimes is not of the concern, here. In particular, the self-sustained oscillation in the unstable-locking region generates the multiple sidebands with the equal frequency separation (Fig. 4-⑤). We believe that this multiple sidebands will be useful in the optical generation of mm-wave signals, which is discussed in more detail in Section IV-C.



Table 1. Simulation parameter values of the laser [14]

Symbol	Parameter	Value
$\lambda$	lasing wavelength	1550 nm
$\Gamma$	confinement factor	0.4
$n_t$	transparent carrier density	$1.0 \times 10^{18}$ [cm <sup>-3</sup> ]
$\tau_p$	photon lifetime	$3.0 \times 10^{-12}$ [sec]
$\tau_n$	carrier lifetime	$1.0 \times 10^{-9}$ [sec]
$\beta$	spontaneous emission factor	$3.0 \times 10^{-5}$
$v_g$	group velocity	$8.5 \times 10^9$ [cm/sec]
$L_a$	cavity length	$300 \times 10^{-4}$ [cm]
$g_0$	differential gain	$12.75 \times 10^{-7}$ [cm <sup>3</sup> /sec]
$\epsilon$	gain suppression factor	$12.75 \times 10^{-7}$ [cm <sup>-3</sup> ]
$V_a$	volume of active layer	$1.5 \times 10^{-10}$ [cm <sup>3</sup> ]
$\alpha$	linewidth enhancement factor	5
$\eta_{ex}$	LD differential quantum efficiency	0.4
$D$	fiber dispersion	17 ps/km/nm
$\eta_{PD}$	PD quantum efficiency	0.8
$I_0$	dark current in PD	$10 \times 10^{-9}$ A
$S_T^2$	thermal noise	$9 \times 10^{-15}$ A <sup>2</sup>

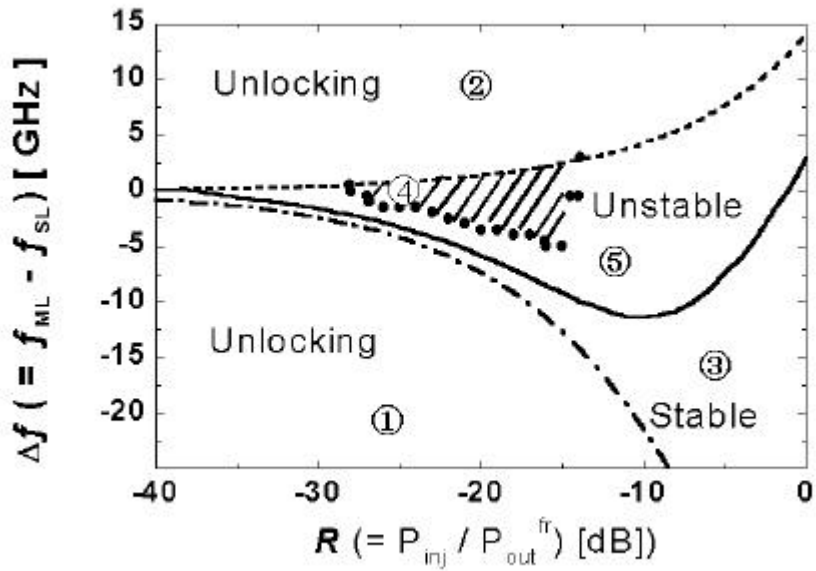
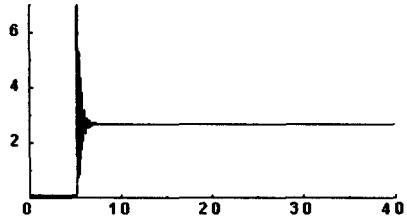
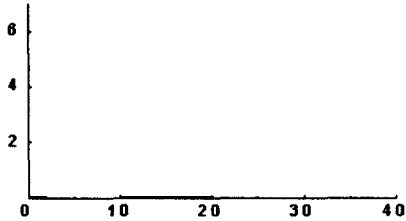


Figure 2. Characteristics of locking regimes. They are characterized into three regimes – unlocking, unstable locking, and stable locking. The shaded area inside the unstable locking regime denotes the place where the chaos occurs. The chaos area outside the locking regimes is not taken into account, here.

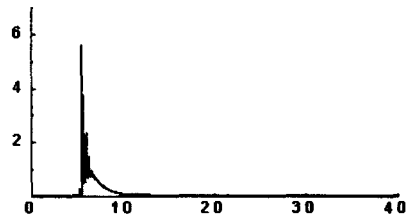
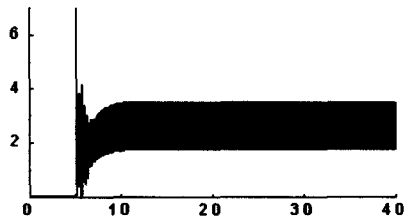
Locked Power [mW]

Unlocked Power [mW]

① Unlocking (lower)



② Unlocking (upper)



③ Stable locking

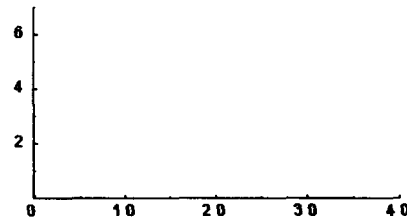
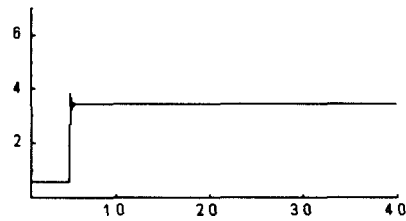
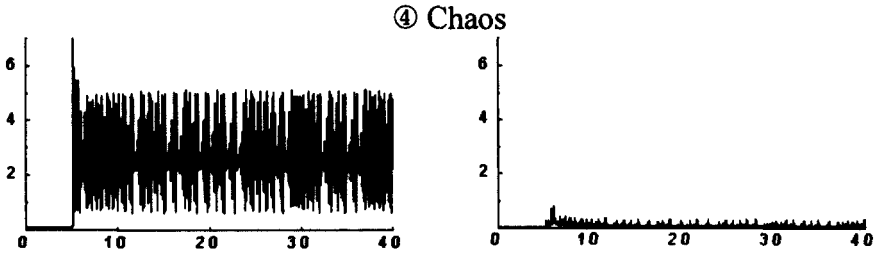


Figure 3. Transient solution of the lasers at different locking conditions, ①~③ in Fig. 2: ①  $R = -25$  dB,  $\Delta f = -20$  GHz, ②  $R = -20$  dB,  $\Delta f = 10$  GHz, ③  $R = -5$  dB,  $\Delta f = -15$  GHz.

Locked Power [mW]

Unlocked Power [mW]



④ Unstable locking

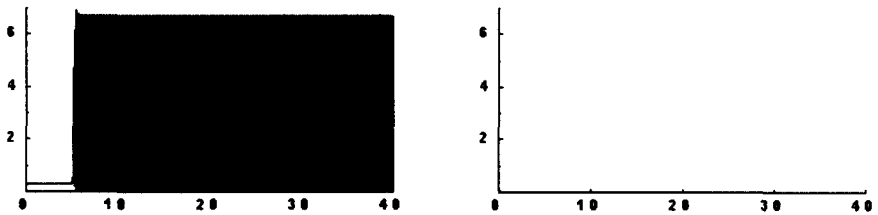


Figure 3. (continued) Transient solution of the lasers at different locking conditions, ①~⑤ in Fig. 2: ④  $R = -28$  dB,  $\Delta f = 0$  GHz, and ⑤  $R = -10$  dB,  $\Delta f = -5$  GHz.

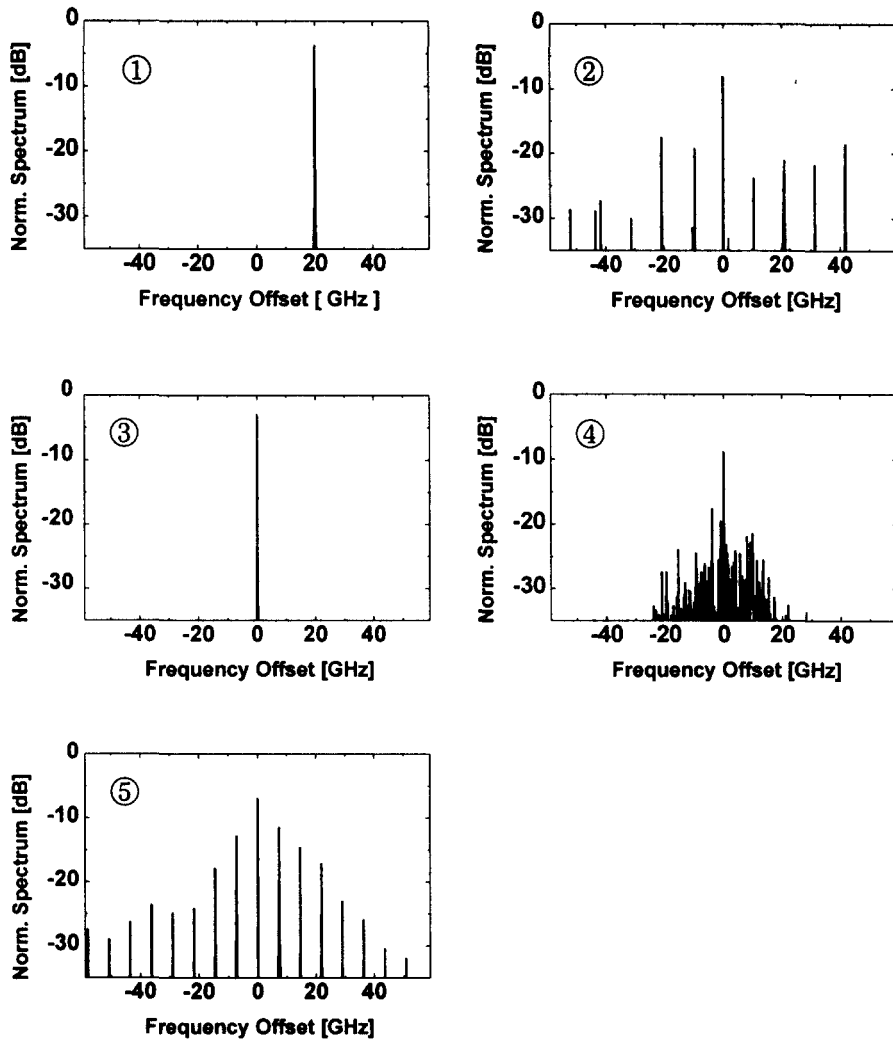


Figure 4. Spectral responses of the laser at the different locking conditions, ①~⑤ in Fig. 2: ①  $R = -25$  dB,  $\Delta f = -20$  GHz, ②  $R = -20$  dB,  $\Delta f = 10$  GHz, ③  $R = -5$  dB,  $\Delta f = -15$  GHz, ④  $R = -28$  dB,  $\Delta f = 0$  GHz, and ⑤  $R = -10$  dB,  $\Delta f = -5$  GHz.

### III. OIL Modulation Response

One advantage of semiconductor lasers is that they can be directly current-modulated. Their modulation speed is limited by the intrinsic modulation bandwidth because the modulation efficiency drops sharply beyond the modulation bandwidth. Moreover, the direct modulation of the lasers leads to the frequency modulation (FM) as well as amplitude modulation (AM) simultaneously. From Eq. 2, one can find that the FM characteristics are directly related with the line-width enhancement factor,  $\alpha$ , and make the laser lasing frequency shift during the modulation. This is the frequency chirp. The chirp is one important parameter to be considered carefully, since the laser chirp, combined with the fiber dispersion, broadens the optical pulse under modulation and acts as the limiting factor in the optical transmission system performance. One method for overcoming the limited modulation bandwidth as well as chirp problem is using the optical injection locking. This section deals with the modulation response and chirp features of the lasers with injection locking.

#### A. Small-Signal Modulation

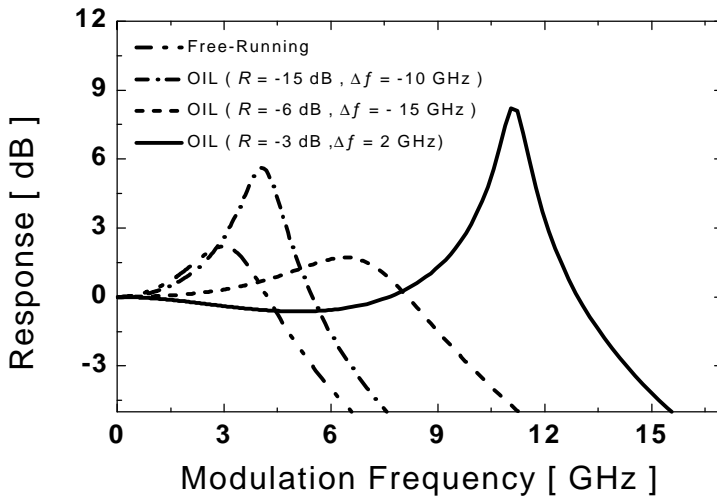
Through the small-signal analysis of Eq. 1~3, the third order system function of the laser with injection locking can be obtained, where as the free-running laser has the second order system function [4]. The derivation method of the OIL system function is identical to those in [13]. Fig. 5-a shows the amplitude modulation responses over modulation frequency for the free-running laser as well as the lasers with injection locking, when SL output power is assumed 2 mW. From Fig. 5-a, the resonance peak of the laser with injection locking ( $R = -3$  dB,  $\Delta f = 2$  GHz) is considerably enhanced up to 11 GHz from the free-running value of 3 GHz. Fig. 5-a shows clearly that the modulation bandwidth can be enhanced with increasing  $R$ .

Fig. 5-b shows the amplitude modulation response with varying  $\Delta f$  for the same  $R$  ( $= -3$  dB). One can see that the upward shift of ML's lasing frequency within the stable locking range can improve the modulation response. Therefore, the modulation characteristics of the lasers with injection locking can be described as functions of the injected power and frequency difference as in Fig. 5. Fig. 6 shows the 3dB-modulation bandwidth normalized by the intrinsic one for three different injected powers ( $R = -13, -6,$  and  $-3$  dB) within each allowed stable locking range. From Fig. 6, one can expect the modulation bandwidth of more than  $2.5\times$  the intrinsic one with the proper control of the injected power and frequency difference.

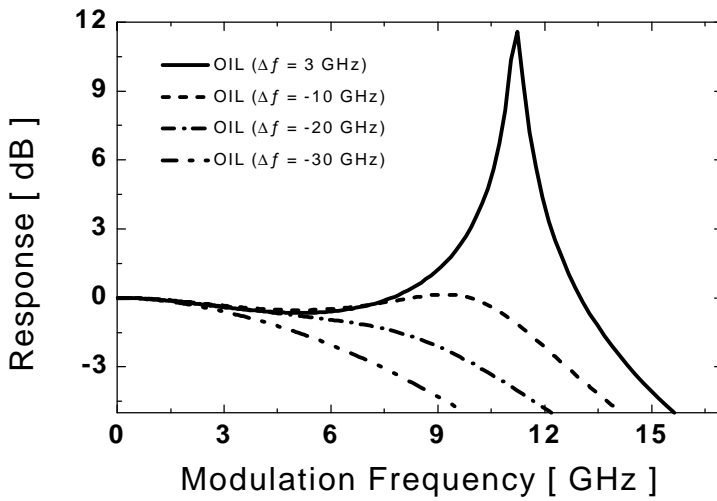
The frequency chirp can be understood through a small-signal analysis as well. Because the frequency chirp is dependent upon the device emitting power, the chirp-to-power ratio (CPR) is adopted [16], where the frequency deviation or chirp is normalized with power as

$$CPR \equiv \frac{|\mathbf{w}\tilde{\mathbf{f}}(\mathbf{w})|}{|\tilde{p}(\mathbf{w})|} \quad (5)$$

The dependence of the frequency chirp on the power is discussed in more detail in Section III-C. In Eq. 5,  $\tilde{p}(\mathbf{w})$  and  $\tilde{\mathbf{f}}(\mathbf{w})$  are the intensity and phase modulation responses respectively, obtained from the small-signal analysis of Eq. 1~3. Fig. 7 shows CPR over modulation frequency for varying  $R$  (Fig. 7-a) and  $\Delta f$  (Fig. 7-b) when the laser output is again assumed 2 mW. From Fig. 7-a, one can see that the CPR of the lasers with injection locking can be improved by around 3 dB ( $R = -15$  dB) to 11 dB ( $R = -3$  dB), when modulated at 5 GHz. Even for the same amount of the injected power ( $R = -3$  dB), Fig. 7-b shows that the CPR can be enhanced by 11 dB ( $\Delta f \approx 5.1$  GHz) from 0.6 dB ( $\Delta f \approx -51.7$  GHz), through the proper tuning of ML lasing frequency. Therefore, similar to the bandwidth enhancement above, one should also understand the CPR improvement as functions of the injected power and the frequency



(a)



(b)

Figure 5. The dependence of the amplitude modulation response on (a) injected power and (b) frequency offset.



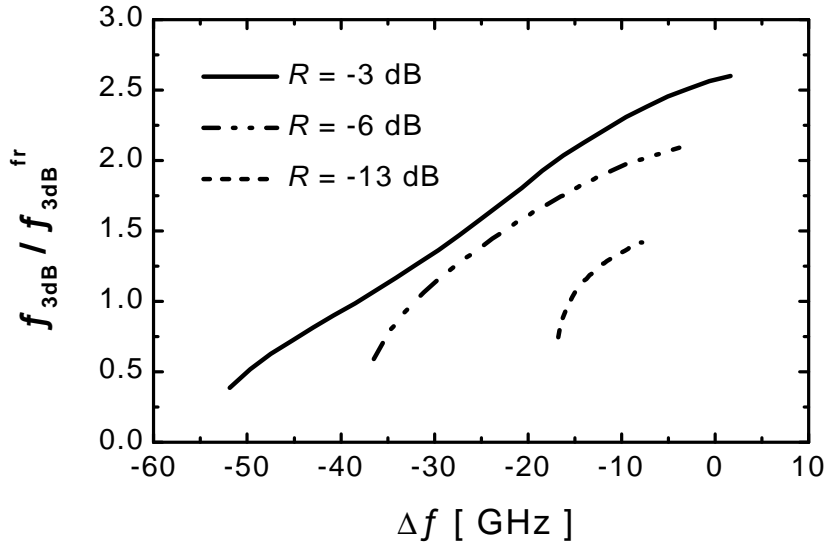
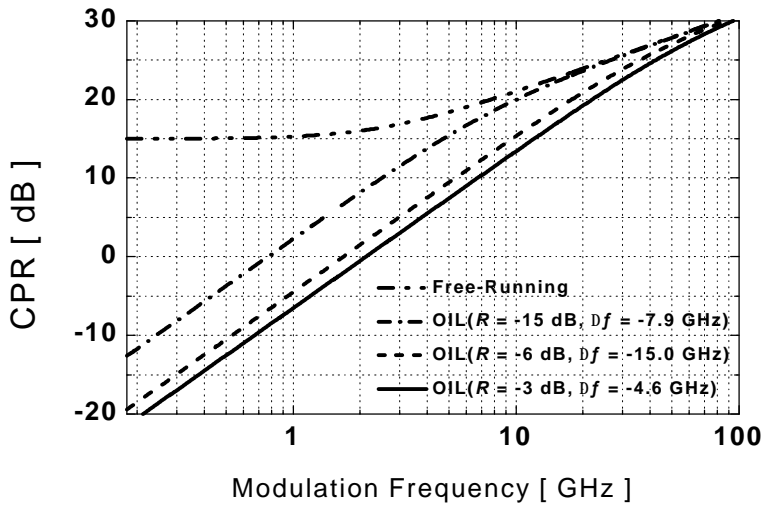
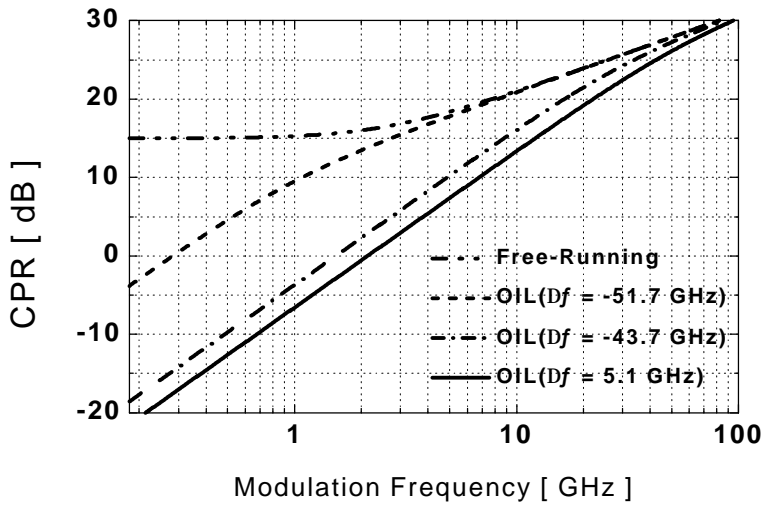


Figure 6. OIL modulation bandwidth normalized by the intrinsic modulation bandwidth within the stable-locking region for different  $R$ 's.



(a)



(b)

Figure 7. The dependence of frequency chirp on (a) the injected power, and (b) the frequency offset.

difference, and can expect the large chirp reduction through the proper control of the locking conditions.

Although the modulation bandwidth enhancement and the chirp reduction are obtained numerically as seen in Fig. 5 ~ 7, their analytical expressions are still under study.

## B. Large-Signal Modulation

The small-signal analysis of the modulation response is very useful in predicting the laser performance, but is not valid for the modulation index of over 0.3 [17]. In order to see the modulation response for the modulation index over 0.3, one should solve the rate-equations, Eq. 1~3, numerically. The fourth order Runge-Kutta integration method is, here, used for the large-signal analysis. Fig. 8 shows the transient output power (solid line) and chirp (dotted line) for (a) free-running (no injection) and (b) injection-locked ( $R = -3$  dB,  $\Delta f = -10$  GHz) lasers. The transmission speed is assumed at 2.5 Gbps in both cases. The bit sequence used for simulation is  $\{1, 0, 1, 1, 1, 0, 0\}$ . From Fig. 8, one can see that OIL can provide significant reduction in the lasing frequency chirp. From Eq. 2, the frequency chirp,  $\mathbf{dn}$ , can be expressed as

$$\mathbf{dn} = \frac{1}{2\mathbf{p}} \frac{d\Phi}{dt} = \frac{\mathbf{a}}{4\mathbf{p}} \left[ \Gamma g_0 (N - n_i) - \frac{1}{\mathbf{t}_p} \right] - \Delta f + \frac{K_C}{2\mathbf{p}} \sqrt{\frac{P_{in}}{P}} \sin(\Phi_{ML} - \Phi). \quad (6)$$

With the approximation of  $g_0/(1+eP)$  in Eq. 1 by  $g_0(1-eP)$ , Eq. 6 can be arranged as

$$\mathbf{dn} = \frac{\mathbf{a}}{4\mathbf{p}} \left[ \frac{1}{P} \frac{dP}{dt} + e\Gamma g_0 (N - n_i) P - \frac{\mathbf{b}\Gamma N}{\mathbf{t}_n P} \right] - \left\{ \Delta f + \frac{K_C}{2\mathbf{p}} \sqrt{\frac{P_{in}}{P}} [\mathbf{a} \cos(\Phi_{ML} - \Phi) - \sin(\Phi_{ML} - \Phi)] \right\}. \quad (7)$$

This equation shows that the frequency chirp for a laser with an external light injection has contributions from the external light (braces) as well as the usual

dynamic (first term of brackets) and DC chirp (second and third terms of brackets). The equation without the light injection terms,  $P_{in}$  and  $\Delta f$ , is identical to the chirp expression of the free-running laser [17]. It is easy to see from the second term in the braces of Eq. 7 that  $dn$  can be reduced by the introduction of external light. Another contribution for chirp reduction comes from the reduction of carrier density with the external light injection. This point becomes clear from the steady-state solution for the carrier density as given below:

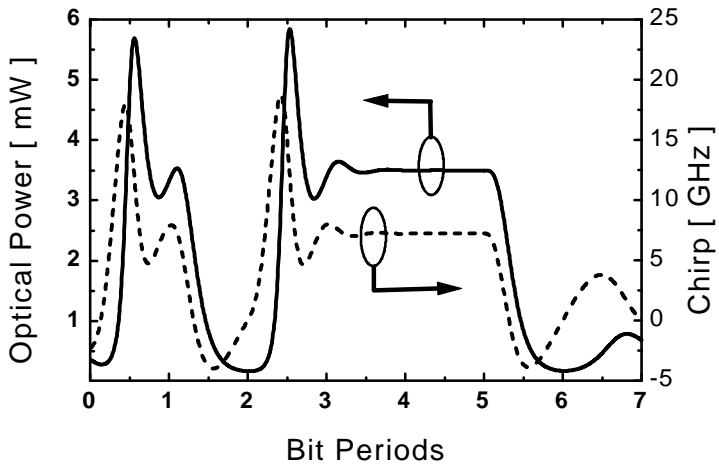
$$N = \left[ \Gamma g_0 (1 - eP) n_i + 1/t_p - 2K_C \sqrt{\frac{P_{in}}{P}} \cos(\Phi_{ML} - \Phi) \right] / \left[ \Gamma g_0 (1 - eP) + \frac{\Gamma b}{t_n P} \right] \quad (8)$$

in which the steady-state carrier density is reduced with  $\sqrt{P_{in}}$ .

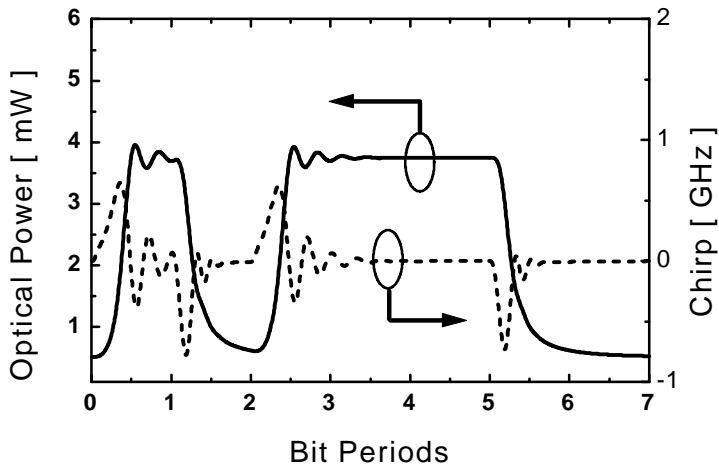
The free-running laser shows the combined effect of the dynamic and DC chirps as seen in Fig. 8-a. The laser lasing frequency shifts instantaneously up toward the high-frequency (blue) and down toward the low-frequency (red) near the up- and down-edges of the optical pulses. Moreover, there exists a large lasing frequency difference between on and off states. For the injection-locked laser, however, the DC frequency difference between on and off states is not observed. Due to the suppression of chirp, the laser with injection locking generates less optical sidebands during the direct current modulation. Hence, the free-running laser shows the multi-longitudinal-mode spectral envelope, but injection-locked SL shows the single-longitudinal-mode spectral envelope with sufficient side-mode suppression [7, 8, 18], when the lasers are directly modulated.

### C. Rf-Modulation Properties

The rf-modulation of the semiconductor lasers (Fig. 9) provides not only amplitude (or, intensity) modulation (AM), but also frequency modulation (FM) simultaneously. To relate AM with FM, the frequency deviations over



(a)



(b)

Figure 8. The transient solutions of the rate equations for (a) free-running, and (b) injection-locked ( $R = -3$  dB) lasers, where the modulation bit rate and extinction ratio are 2.5 Gbps and 7, respectively. The solid lines represent optical powers, and dotted lines frequency chirps.

modulation frequency are examined in Fig. 10 with varying the biasing conditions. The derivation method of the maximum frequency deviation is identical to those in [17]. From its derivation, one can see that it is directly proportional to the linewidth enhancement factor,  $\alpha$ . Fig. 10 shows the increase of the resonance frequency and the decrease of the maximum frequency deviations, when increasing the biasing point and emitting power. Therefore, the frequency deviation (or, chirp) has the power-dependency.

The spectral analysis of the laser under one-tone rf-modulation is also performed with varying the modulating current amplitude. The field of the laser under one-tone rf-modulation is expressed [19] by

$$E(t) = E_0 \exp\{j[2\mathbf{p}\mathbf{n}_0 t + \mathbf{b} \cos(2\mathbf{p}\mathbf{n}_{RF} t) + \Phi(t)]\} \quad (9)$$

where  $\nu_0$  is the laser lasing frequency,  $\mathbf{b} = \mathbf{n}_d / \mathbf{n}_{RF}$  FM index,  $\nu_{RF}$  modulation frequency, and  $\Phi$  random phase fluctuations of the optical carrier. Eq. 9 can be decomposed into Fourier components,

$$E(t) \propto \left[ \sum_{n=-\infty}^{\infty} J_n(\mathbf{b}) \exp[j2\mathbf{p}(\mathbf{n}_0 + n\mathbf{n}_{RF})t] \right] \exp[j\Phi(t)] \quad (10)$$

where  $J_n$  is the Bessel functions of the first kind of order  $n$ . The power spectrum of Eq. (10) is

$$S(f) \propto \left[ \sum_{n=-\infty}^{\infty} \mathbf{d}(\mathbf{n}_0 + n\mathbf{n}_{RF}) \right] \otimes S_l(\mathbf{n}) \quad (11)$$

where  $\otimes$  indicates the convolution, and  $S_l(\nu)$  the Lorentzian spectral lineshape of the laser emission.

Fig. 11 shows the spectra of the laser under rf-modulation with varying the peak-to-peak modulating current amplitude,  $I_{p-p}$ , when  $I_{DC} = 1.5 \times I_{th}$  and  $\mathbf{n}_{RF} = 2$  GHz. Under modulation, the spectra is asymmetric and becomes broadened with increasing  $I_{p-p}$ . One should also note that the fundamental spectral peak at  $\mathbf{n}_0$  can be suppressed by the control of  $I_{p-p}$ . The spectral broadening under

modulation is combined with the fiber dispersion and broadens the optical pulse, resulting in the degradation of the overall optical transmission performance. One method of reducing the extent of the spectral broadening is using OIL technique, since OIL reduces the frequency chirp, as discussed above, and hence results in the suppression of the spectral broadening under modulation as well as the improvement in the system performance. The influence of OIL on the fiber-optic transmission performance is discussed in Section IV-A.

Moreover, the chirp reduction and suppression of the spectral broadening by OIL can be understood as the suppression of the nonlinear properties, which is one major concern in the optical analog communication [20] and is also examined in Section IV-B. In the contrast, the spectral broadening is very useful in the optical generation of  $\mu$ - / mm- signals, when the FM sideband injection locking method is employed [12, 19, 21]. This is discussed in Section IV-C, as well.

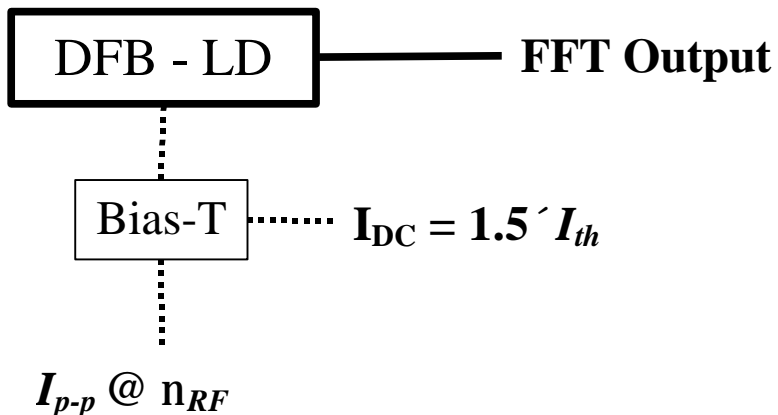


Figure 9. Simulation block diagram for the laser under rf-modulation.  $I_{DC}$  is the biasing current,  $I_{p-p}$  the peak-to-peak modulation current amplitude, and  $n_{RF}$  the modulation frequency of the applying sinusoidal wave.



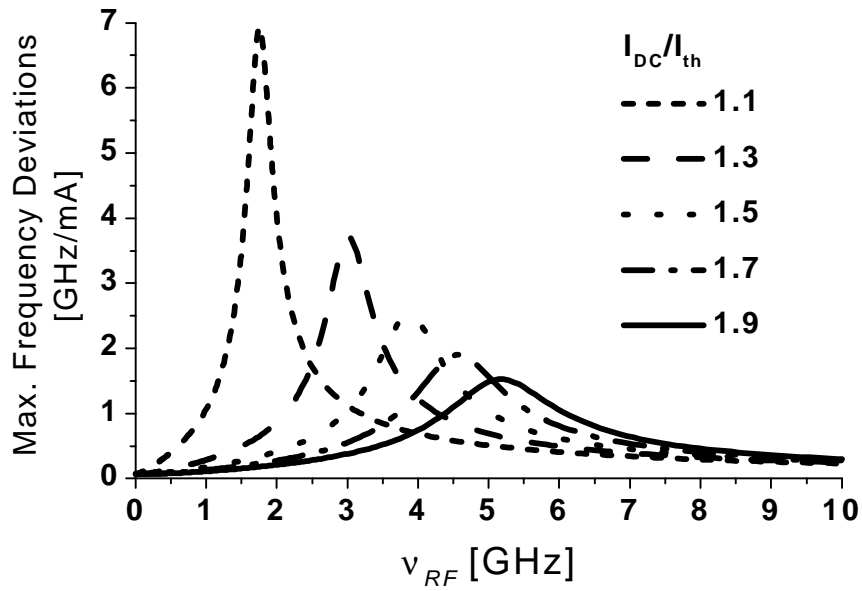


Figure 10. The frequency response of the maximum frequency deviations for the different bias currents, which has the peak value at the laser resonance frequency.

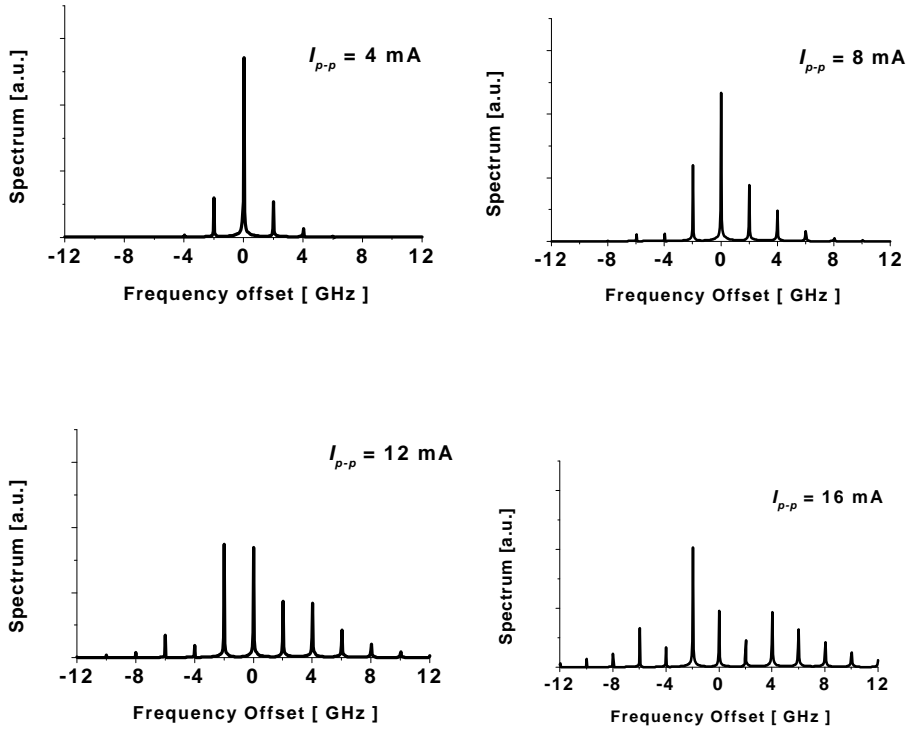


Figure 11. Optical spectra of the field of the laser with varying the modulating current amplitude,  $I_{p-p}$ . The laser is assumed to be biased at  $1.5 \times I_{th}$ , where  $I_{th} = 33.5 \text{ mA}$ , here. The laser output can be obtained by integrating the rate-equations.

## IV. OIL Applications

The overall characteristics and modulation responses of the semiconductor lasers with injection locking have been examined. The OIL technique can be utilized in the various applications, since it improves the laser characteristics (i.e., modulation bandwidth enhancement, chirp / noise reduction, and suppression of nonlinear distortion). The purpose of this section is to relate the influence of optical injection with the system performance in applications.

### A. Fiber-Optic Transmission

Although the direct current modulation of semiconductor lasers is simple and compact, it is not suitable for high-capacity, long-distance fiber-optic transmission applications. It is because the lasing frequency chirp during the direct current modulation, coupled with the fiber dispersion, can cause severe system performance degradation. This degradation becomes more serious when the transmission speed increases. One method of overcoming this problem is using the optical injection locking (OIL) technique. Fiber-optic transmission experiments using an injection-locked semiconductor laser have been successfully demonstrated for transmitting 140 Mbps and 445.8 Mbps signals for 102 km and 170 km respectively [7-8], but no reports have been made that systematically investigate the influence of injection locking on the transmission performance.

This subsection deals with the characteristics of injection-locked semiconductor lasers and their influence on the transmission performance. A model fiber-optic transmission system used for our study is shown in Fig. 12. The system configuration and the analysis method are identical to those in [14] except for the following three points:

- 1. The transmitting laser is injection-locked by an external laser.*
- 2. A p-i-n photo-detector is used instead of APD.*

3. *The truncated pulse train Gaussian approximation method for BER estimation is used instead of the truncated pulse train Gaussian quadrature rule method.*

The number of bits,  $M$ , interfering with decision process is taken 2, here. For the bit sequences,  $2^{2M+1}$ , each probability of error is summed up and averaged out to produce the average BER. The decision time is determined at which the filtered current pattern for the bit sequence {00100} gives the maximum eye opening. The decision threshold is optimized for the best BER at that decision time.

For the numerical analysis, the SL average emitting power is limited at 3 dBm in order to avoid undesired nonlinear effects in the fiber [22]. The frequency difference is also assumed - 10 GHz, which guarantees stable locking for both on- and off- states as long as  $R \geq -13$  dB. The applied current input in NRZ format is assumed to have the rising and falling times of  $0.25 \cdot T$ , where  $1/T$  is the modulation speed. The SL emitting optical power and phase can be obtained through the Runge-Kutta integration of the rate-equations, Eq. 1 ~ 3.

Fig. 13 shows the average BER curves for free-running (no injection) and injection-locked ( $R = -13$  dB and  $-3$  dB,  $\Delta f = -10$  GHz) lasers at 2.5 Gbps, extinction ratio of 7 for 100 km of fiber. The extinction ratio,  $g_{ex}$ , is defined as the ratio of on- state and off- state power. Clearly, OIL enhances the system performance. At BER of  $10^{-9}$ , injection-locked lasers have the receiver sensitivity of - 30.3 dBm with  $R = -3$  dB and - 29.5 dBm with  $R = -13$  dB, whereas the free-running laser has the receiver sensitivity of - 28.5 dBm. This attributes to chirp reduction in injection-locked lasers.

The combined effect of laser chirp and fiber dispersion is clearly illustrated in Fig. 14, where the dependence of the receiver sensitivity on the fiber-optic length up to 100 km is shown for 2.5 Gbps, and  $g_{ex}$  of 9. After 100km of fiber, free-running lasers have power penalty of 2.8 dB whereas injection-locked lasers have 0.1 dB for  $R = -3$  dB. The laser with injection locking ( $R = -3$  dB,

$\Delta f = -10$  GHz) is very insensitive to the fiber dispersion and can offer less power penalty. It is due to the reduced dynamic chirp by the strong damping as well as the reduced DC chirp by the less carrier density as discussed in Section III-B.

Fig. 15 shows the dependence of the receiver sensitivities on  $g_{ex}$  at 2.5 Gbps for 100 km of fiber. As discussed in [14, 23], the ordinary free-running laser has an optimal  $g_{ex}$  due to a tradeoff between the large chirp at the high  $g_{ex}$  and the poor receiver sensitivity at the low  $g_{ex}$ . However, the receiver sensitivity of lasers with injection locking ( $R = -3$  dB) improves with increasing  $g_{ex}$ , and gets saturated to the receiver sensitivity of  $-30.6$  dBm, respectively, while the free-running laser has around  $-28.5$  dBm even at the optimal  $g_{ex}$ .

The dependence of the receiver sensitivity on the transmission speed is shown in Fig. 16, where the fiber length and  $g_{ex}$  are assumed 100 km and 9. The system performance gets severely degraded as the transmission speed increases. It is because the increased rate of output power change at higher modulation speeds causes more severe transient chirp. The performance of an injection-locked laser is, however, less dependent on the modulation speed. It results from the enhanced modulation bandwidth and reduced frequency chirp as discussed in Section III-A. From the numerical analysis, it is found that the free-running laser can be modulated up to 3 Gbps achieving BER's of  $10^{-9}$  or less, but injection-locked lasers can be modulated up to 8 Gbps for  $R = -3$  dB.

Therefore, optical injection locking technique can be advantageous for the high-capacity long-span fiber-optic transmission system. When using optical injection locking technique, the transmission span is limited only by fiber loss. Future works will focus on the experimental implementation of strong optical injection locking to prove the transmission performance enhancement.

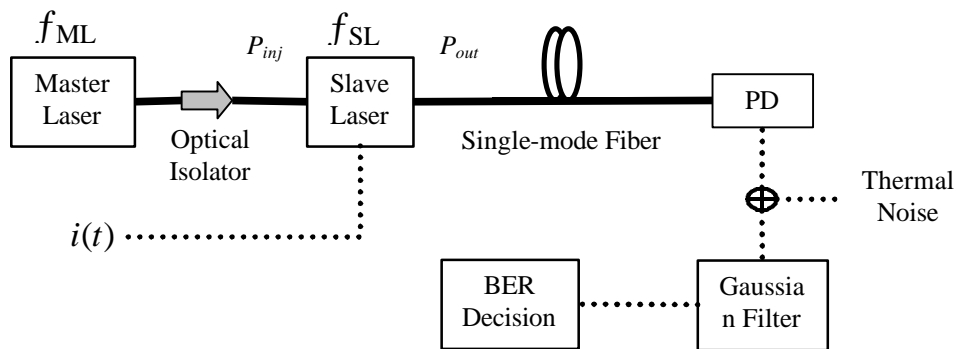


Figure 12. Schematic of numerical simulation, The applied current into SL is in NRZ modulation format with the rising time of  $0.25/T$ , where  $1/T$  is the modulation speed. The solid line represents the optical path and the dotted one the electrical path. Optical fibers is modeled as a filter. The receiver filter is assumed Gaussian.

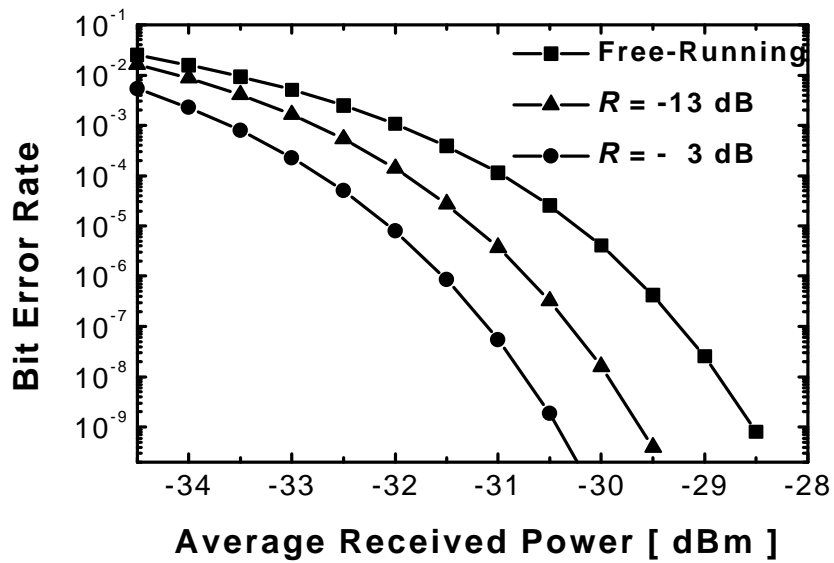


Figure 13. BER curves for the free-running (no injection) and injection-locked ( $R = -13$  dB and  $-3$  dB) lasers, transmitted at 2.5 Gbps. The extinction ratio and fiber-optic length are 7 and 100 km, respectively.

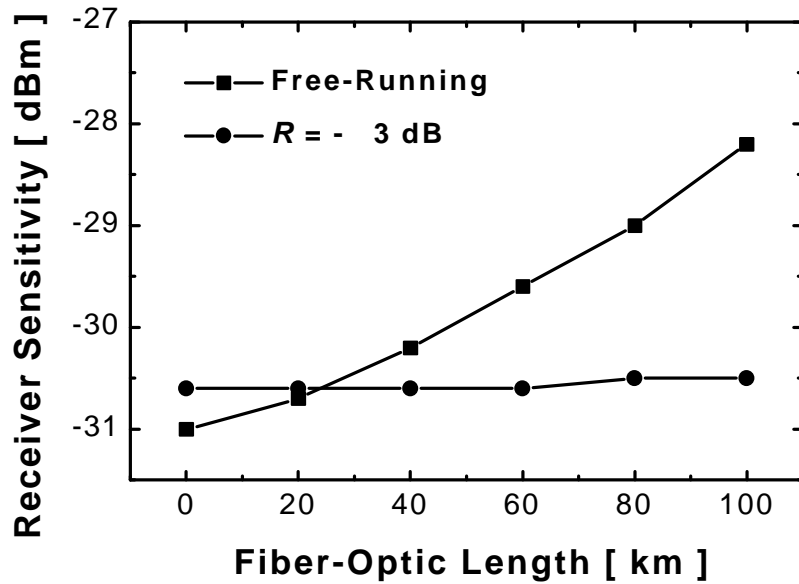


Figure 14. Dependence of the receiver sensitivity on the fiber-optic length, transmitted at 2.5 Gbps with the extinction ratio of 9. In the computer simulation, the power penalties due to the fiber dispersion are 2.8 dB (free-running, square), and 0.1 dB ( $R = -3$  dB, circle).



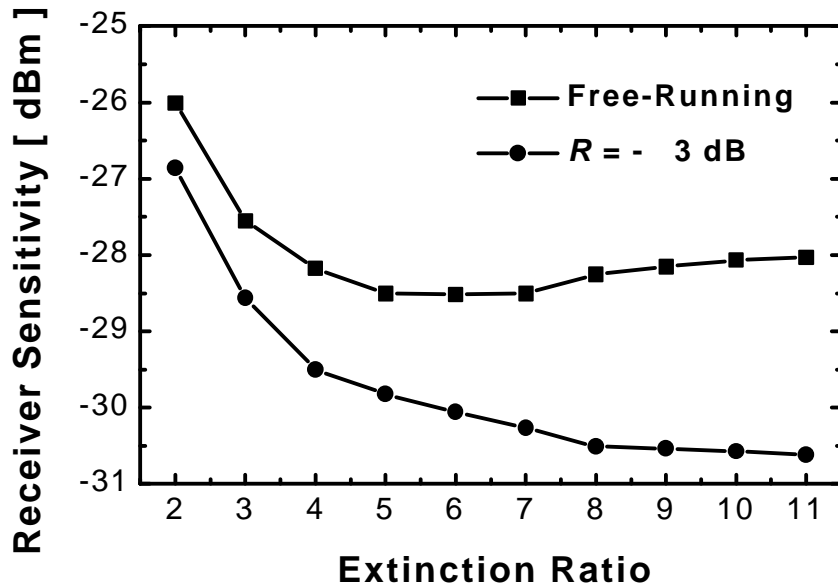


Figure 15. Dependence of the receiver sensitivity on the extinction ratio, transmitted at 2.5 Gbps after fiber-optic length of 100 km. The free-running laser has the optimal extinction ratio of 6. The injection-locked lasers can offer the better receiver sensitivities at the large extinction ratios. The value of dispersion parameter used in the simulation is 17 ps/nm/km.

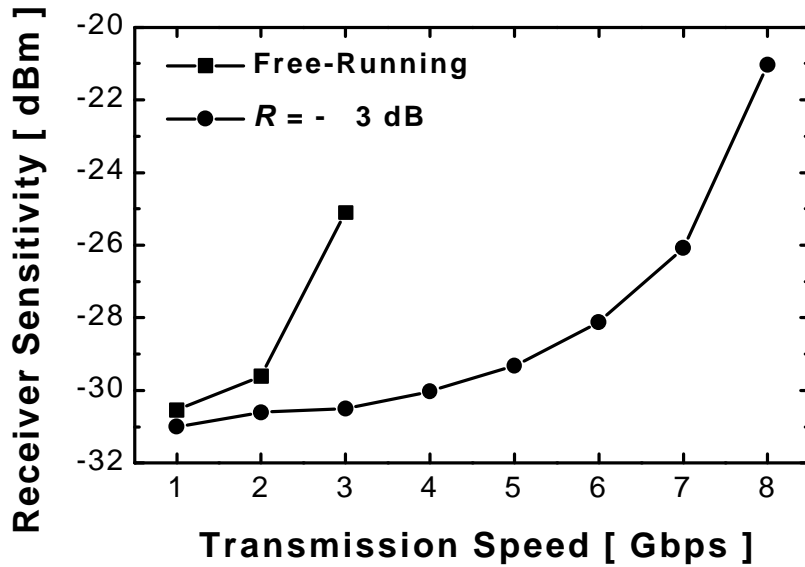


Figure 16. Dependence of receiver sensitivity on transmission speed. When the transmission speed of the free-running laser is limited to 3 Gbps, the lasers with injection locking ( $R = -3$  dB) can be transmitted up to 8 Gbps. This results from the enhanced modulation bandwidth in presence of optical injection as seen in Fig. 5.

## B. Optical Analog Transmission

The optical analog transmission of GHz-range signals is recently attracting much interest for WLL (wireless local loop), CATV, and satellite system applications. In these applications, direct modulation of a semiconductor laser diode (LD) is used for transmitting signals multiplexed by RF-range sub-carriers. Consequently, the LD non-linearity becomes a key issue in the system performance because it can impose signal distortions by inter-channel interference, which limit the number of channels as well as transmission distance [20, 24].

In this subsection, the numerical analysis of injection-locked lasers is performed to show that OIL improves LD non-linear characteristics and experimentally confirm it. It is believed that this confirmation is done for the first time. The basic block diagram for the experiment setup is illustrated in Fig. 17. The numerical analysis of injection-locked lasers is based on Lang's equations [25] in which the laser nonlinear characteristics are described with the gain suppression term in the rate equations. The simulation parameters are obtained from [14]. For the simulation, two rf-sources ( $f_1 = 2.5$  GHz and  $f_2 = 2.7$  GHz) with the same amplitude ( $I_{rf}$ ) are used in order to directly modulate the SL. The SL output spectrum is obtained by fast-Fourier-transforming the output power of SL laser calculated by the Runge-Kutta integration of Lang's equations.

Fig. 18 shows the amplitudes for fundamental and harmonic components of LD output spectra as function of  $I_{rf}$  for (a) free-running (no optical injection) and (b) injection-locked ( $R = -7.9$  dB,  $\Delta f = -15$  GHz) lasers. The second inter-modulation products (IMPs) at  $f_1+f_2$  and  $2f_1$ , and third IMP at  $2f_2-f_1$  are smaller for injection-locked LD than for free-running LD. The slight difference in the amplitude of the fundamental term ( $f_1$ ) is due to the change in LD dynamic characteristics caused by injection locking. This is shown in Fig. 19

where the amplitudes of several frequency components are compared for the free-running and OIL cases. It is found from Fig. 19 that the external optical injection suppresses the third-order IMP,  $2f_2-f_1$ , by 6~25 dB within the range of 2~4 GHz.

Fig. 20 shows the experimentally measured spectral amplitudes at  $f_1$ ,  $f_1+f_2$ ,  $2f_1$ , and  $2f_2-f_1$  for varying RF currents ( $f_1 = 2.5$  GHz, and  $f_2 = 2.7$  GHz). For the measurement, an external-cavity tunable LD is used for ML and a DFB-LD (Samsung SDL24-B1-3) without isolator is used for SL. SL is dc-biased at  $2 \times I_{th}$  ( $I_{th} = 7$  mA). The input current loss has not yet been quantified due to impedance mismatching. Fig. 20 illustrates LD non-linearity improvement of OIL (estimated  $R = -3$  dB,  $\Delta\lambda = 0.078$  nm) over free-running case. As the applied current is increased, the spectral amplitudes of the free-running laser get saturated because, it is believed, over-modulation clips LD output. In the meanwhile, OIL amplitudes over the same current modulation do not saturate itself. It is believed that this is related with the decrease of LD threshold current with the injection locking [26].

Fig. 21 shows the measured *rf*-spectra for  $I_{rf}$  of 5 dBm. The OIL fundamental modulation product and third IMPs are smaller than free-running ones as expected from the numerical results. Theoretical and experimental results are in the qualitative agreement although the parameters used in the simulation do not reflect the parameters for the LD used in the experiment.

Therefore, the IMP suppression with OIL can find useful applications in optical analog transmission systems. Future works are in progress in order to identify the exact cause for non-linearity reduction with optical injection.

### C. Optical Generation of mm- wave signals

The optical generation of mm-wave signals has been attracting much interest, due to the frequency bandwidth shortage problem of existing systems

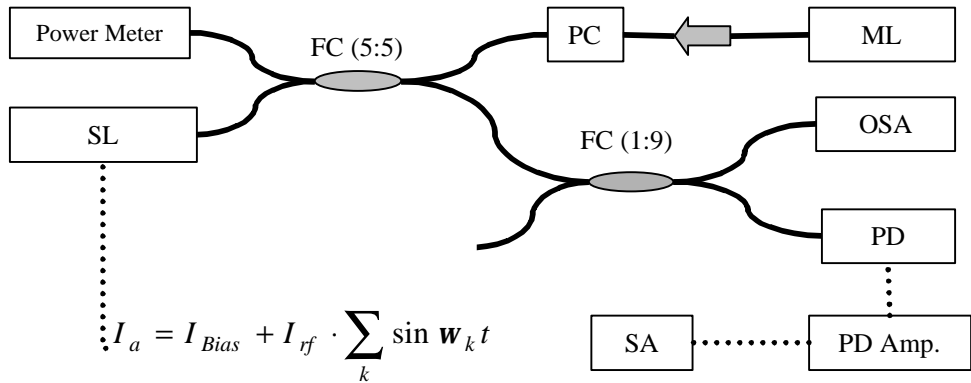


Figure 17. Basic block diagram for the experiment. The external cavity tunable laser and DFB-LD are used for ML and SL, respectively. PC denotes polarization controller, FC fiber coupler, OSA optical spectrum analyzer, PD high-speed photodiode, PD Amp PD amplifier (Gain = 10 dB), and SA spectrum analyzer. The arrow indicates optical isolator (Samsung ISO-A115NO).

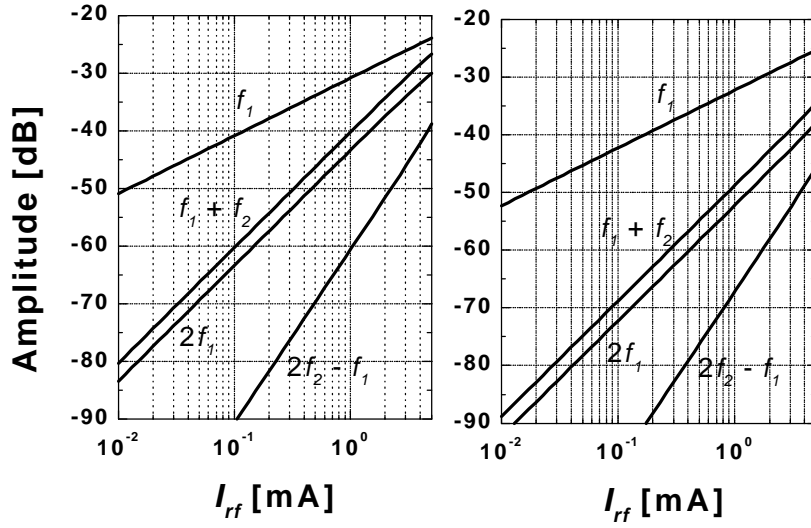


Figure 18. Simulated spectral amplitudes at  $f_1$ ,  $f_1+f_2$ ,  $2f_1$ , and  $2f_2-f_1$  for (a) free-running (no optical injection) and (b) injection-locked ( $R = -7.9$  dB,  $\Delta f = -15$  GHz) lasers ( $f_1 = 2.5$  GHz and  $f_2 = 2.7$  GHz).

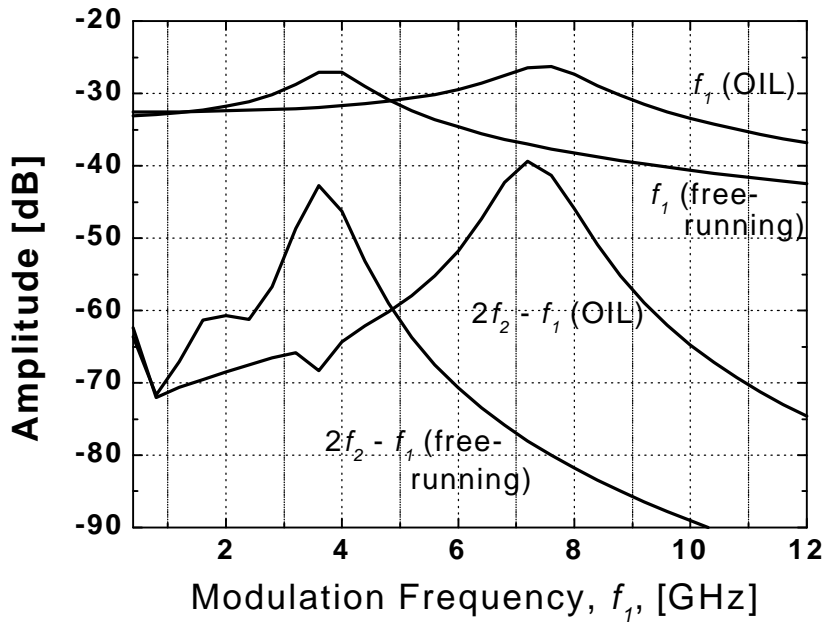


Figure 19. Simulated modulation frequency responses at  $f_1$  and  $2f_2 - f_1$  for free-running and injection-locked lasers ( $f_2 = f_1 + 200\text{MHz}$ ,  $I_{rf} = 1\text{mA}$ ).

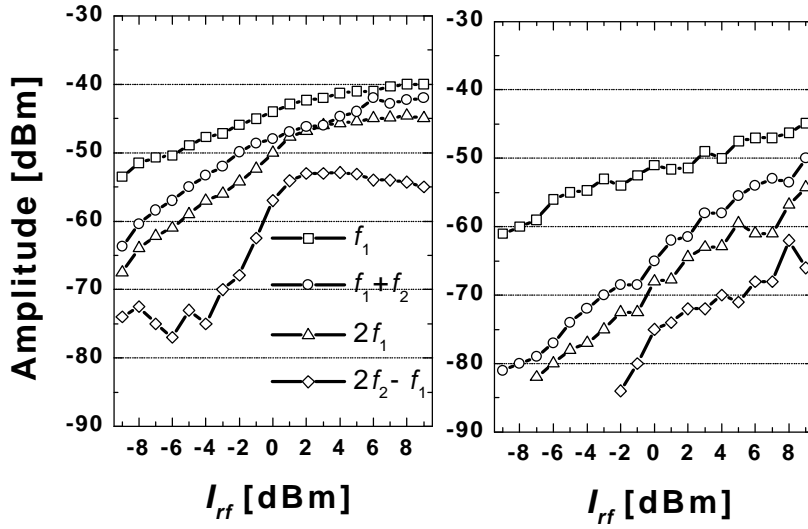


Figure 20. Measured spectral amplitudes of fundamental modulation, and second / third inter-modulation products for (a) free-running and (b) injection-locked ( $R = -3$  dB,  $\Delta f = -9.75$  GHz) lasers ( $f_1 = 2.5$ GHz, and  $f_2 = 2.7$  GHz).



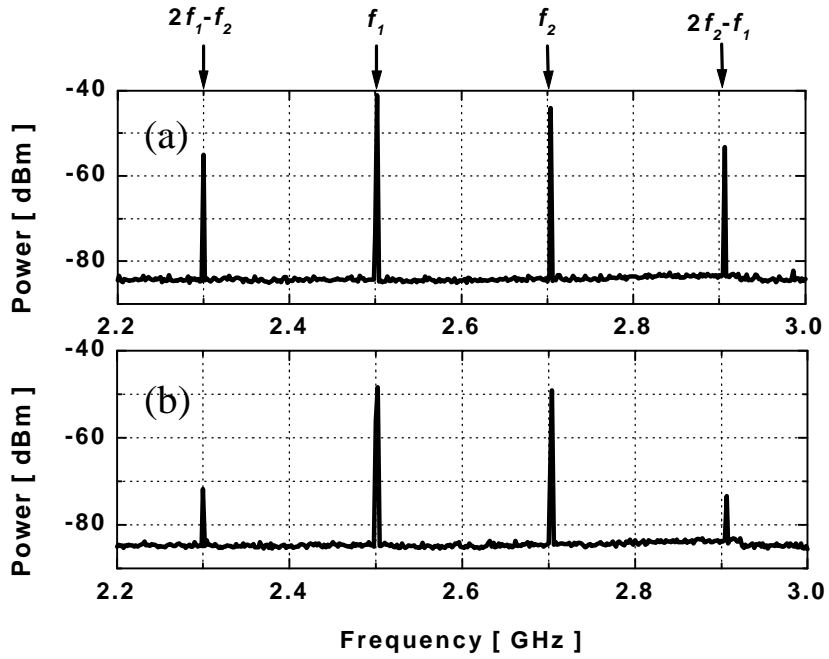


Figure 21. Measured rf-spectra of (a) free-running and (b) injection-locked lasers for  $I_{rf} = 5$  dBm in Fig. 20.

and the urgent need for the high-speed data transmission. The optical generation method can achieve the wide frequency range of carrier signals easily, and is capable of the extremely low loss transmission through the fiber-optic links. Some applications for this method that has been proposed include [20]:

- *satellite communications*
  - *antenna remoting and remote operation of satellite earth stations*
- *mobile radio communication networks*
- *dropwire replacement by radio*
- *braodband access by radio*
- *Multipoint Video Distribution Services (MVDS)*
- *Mobile Broadband System (MBS)*
- *vehicle communications and control*
- *radio LANs over optical networks*

Using the FM sideband injection locking method, Goldberg [19, 21] demonstrated the generation of signals of 10.5 GHz with an electrical linewidth of less than 10 Hz. The basic configuration is illustrated in Fig.22. As discussed in Section III-C, the laser (master laser, ML) under rf-modulation generates the multiple optical sidebands equally spaced with electrical modulating frequency,  $\mathbf{n}_{RF}$ , and its light is injected into another lasers (slave laser, SL). When SL1 and SL2 are injection-locked to the m-th and k-th sidebands, they suppress the other sidebands and can be described by

$$\begin{aligned} E_1 &\propto e^{i[2\mathbf{p}(\mathbf{n}_0+k\mathbf{n}_{RF})t+\mathbf{f}(t)]} \\ E_2 &\propto e^{i[2\mathbf{p}(\mathbf{n}_0+m\mathbf{n}_{RF})t+\mathbf{f}(t)]} \end{aligned} \quad (12)$$

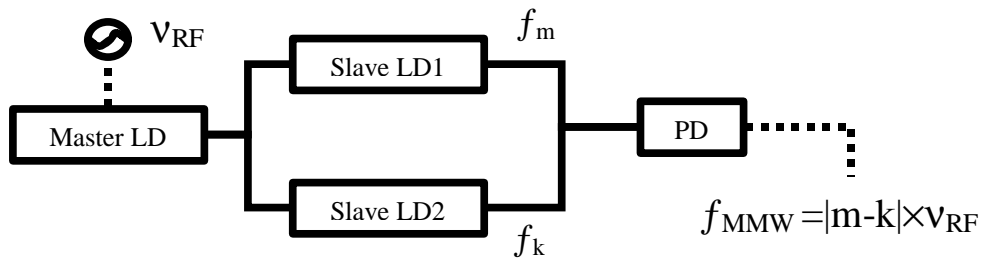
The outputs of SL1 and SL2 is photo-detected and beat each other in the photo-diode (PD), generating the beating current,  $i(t) \propto |E_1 + E_2|^2$ , by

$$i(t) = \mathbf{h}_{PD} \left[ P_1 + P_2 + 2\sqrt{P_1 P_2} \cos(k - m)2\mathbf{p}\mathbf{n}_{RF}t \right] \quad (13)$$

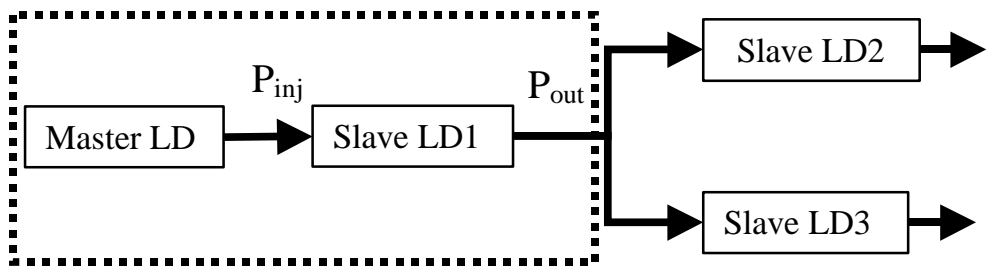
where  $\mathbf{h}_{PD}$  is the PD responsitivity, and  $P_1$  and  $P_2$  are the powers incident on PD from SL1 and SL2. This method is not only dependent on the laser FM response, but also requires an electrical rf-source. Therefore, a technique that does not

require external rf-source would be highly desirable. Realizing such an OIL system is the goal of this subsection.

Recent studies on OIL have found that the modulation bandwidth of a semiconductor laser can be significantly enhanced under the strong optical injection [3-6]. However, the locking properties under the strong optical injection have not been fully analyzed outside the dynamically stable locking range, where such effects as undamped relaxation oscillation and chaos can occur. The analysis of the spectral characteristics of semiconductor lasers under strong optical injection is discussed earlier in Section II-B. It is found that the generation of multiple optical sidebands having large frequency separation is possible. Feeding these sidebands into two SL's, as shown in Fig. 23, it is possible to generate optical  $\mu$ -mm-waves without using any external RF source. As an example, Fig. 24 shows the optical spectra under two different operation conditions outside the dynamically stable locking range. The frequency separations are 7.25 GHz (Fig. 24-a) and 12.6 GHz (Fig. 24-b). If SL2 and SL3 are injection-locked to the  $\pm 4$ -th sidebands of SL1 output, as indicated by arrows in Fig. 24-a and -b, the beat frequencies of 58 GHz and 100.8 GHz can be achievable. In addition, the frequency separation can be controlled by the proper adjustment of the injected power, as shown in Fig. 25. Future works are in progress in order to demonstrate this technique and stabilize the beat frequency.

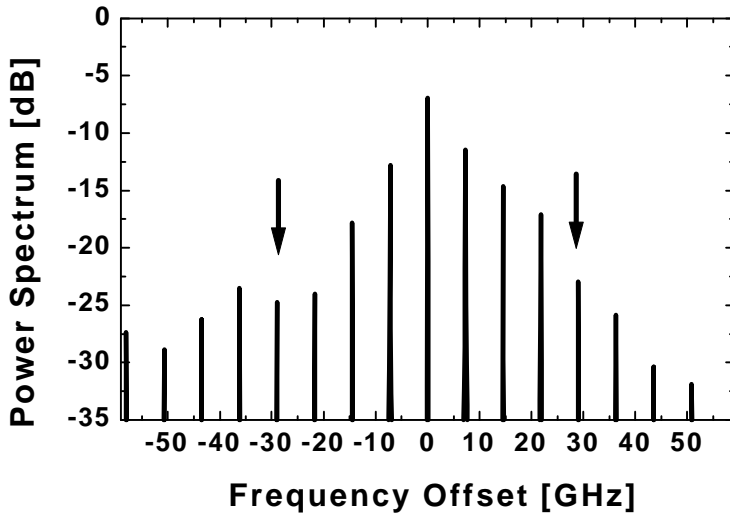


(a)

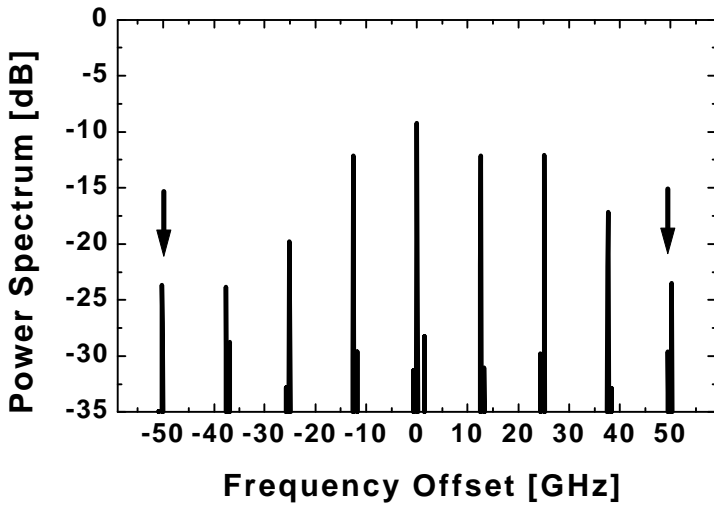


(b)

Figure 22. Block diagrams for (a) the typical and (b) the proposed OIL technique for  $\mu$ - / mm- wave generation



(a)



(b)

Figure 23. Calculated power spectra of the injection-locked lasers in the unstable-locking regime of Fig. 2: (a)  $R = -10$  dB and  $\Delta f = -5$  GHz, and (b)  $R = -5$  dB and  $\Delta f = 5$  GHz.

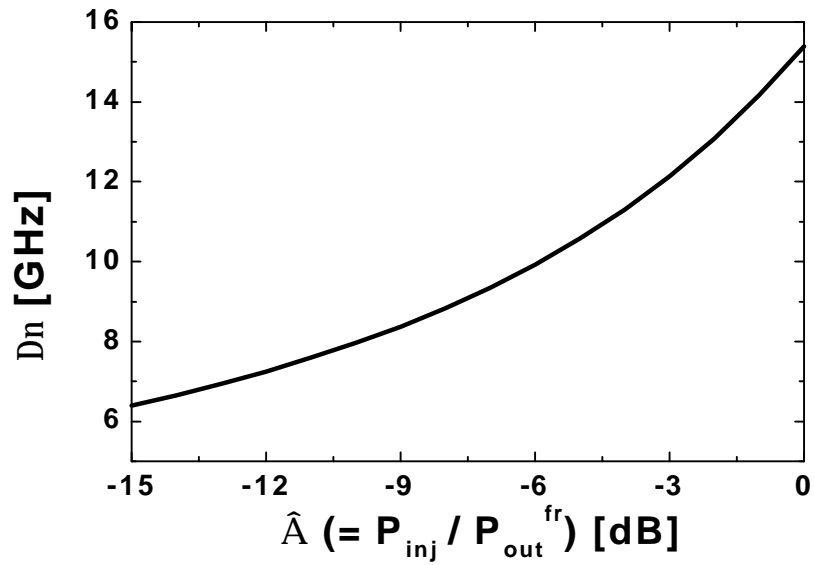


Figure 24. The sideband separation,  $\Delta\nu$ , as a function of  $R$  along the boundary (shown as dashed line) in Fig. 2.

## V. Summary

The characteristics, modulation responses, and applications of the semiconductor laser with injection locking have been investigated. From the steady-state solution of the rate-equations under external optical injection, the locking range can be understood as functions of the injected power and the frequency difference. The locking characteristics are quite different at different locking conditions. In the dynamically stable region, only the MS mode shows up. In the unlocking region, either the SL mode show up dominantly or both SL and MS modes as well as their four-wave mixing conjugates appear depending on the injected power and frequency offset. In the dynamically unstable region, the spectrum can be chaotic or several sidebands separated by equal frequency can show up again depending on the injected power and frequency offset. The sidebands in dynamically unstable region can be quite useful for generating optical microwave signals as they can be injected to additional two SL's and lock them, producing two coherent light signals separated by the desired frequency offset.

From the small-signal and large-signal analysis of the rate-equations, it is found that the optical injection locking can not only enhance the modulation bandwidth, but also reduce the frequency chirp significantly. In addition, the reduction of the frequency chirp, related with the laser FM response, results in the improvement of the nonlinear distortion of the laser under multi-tone rf-modulation. In particular, the nonlinearity improvement of laser with injection locking under two-tone rf-modulation has been experimentally demonstrated.

To relate the influence of the enhanced laser characteristics by OIL with the overall system performance, the dependence of system performance on injected power, transmission length, extinction ratio, and transmission speed is investigated. It is found that optical injection locking technique can be advantageous for the high-capacity long-span fiber-optic transmission system.

When using optical injection locking technique, the transmission span is limited only by fiber loss. The experimental implementation of strong optical injection locking will be made in near future in order to prove the transmission performance enhancement.

As discussed earlier, due to the significant chirp reduction under strong optical injection, it is also found that the IMP suppression with OIL can find useful applications in optical analog transmission systems. And, future works are in progress in order to identify the exact cause for non-linearity reduction with optical injection.

The new optical mm-wave generation method is proposed, using the intrinsic characteristic of the laser under strong optical injection. In the unstable locking conditions, the laser generates the multiple optical sidebands separated by equal frequency. Feeding these sidebands into two SL, it is possible to generate optical  $\mu$ /mm-waves without using any external RF source. In addition, the frequency separation can be controlled by the adjustment of the injected power.

This paper is mainly focused on the theoretical investigation of optical injection locking. This technique can be extended to the various applications - optical switching, optical frequency stabilization, noise suppression and so on. The theoretical extension and experimental implementation remain as future works.



## VI. References

- [1] S. Weisser, E. C. Larkins, K. Czotscher, W. Benz, J. Daleiden, I. Esquivias, J. Fleissner, J. d. Ralston, B. Romero, R. E. Sah, A. Schonfelder, and J. Rosenzweig, "Damping-limited modulation bandwidth up to 40 GHz in undoped short-cavity In<sub>0.35</sub>Ga<sub>0.65</sub>As-GaAs multiple-quantum-well lasers," *IEEE Photon. Tech. Lett.*, vol. 8, no. 5, pp. 608-610, 1996.
- [2] Yasuhiro Matsui, et al., "30 GHz Bandwidth 1.55  $\mu\text{m}$  strain-compensated InGaAlAs-InGaAsP MQW laser," *IEEE Photon. Tech. Lett.*, vol. 9, no. 1, pp. 25-27, 1997.
- [3] G. Yabre, "Effect of Relatively strong Light Injection on the Chirp-to-Power Ratio and the 3 dB Bandwidth of Directly Modulated Semiconductor Lasers," *J. Lightwave Technol.*, vol. 14, no. 10, pp. 2367-2373, 1996.
- [4] J. Wang, M. K. Haldar, L. Li, and F. V. C. Mendis, "Enhancement of Modulation Bandwidth of Laser Diodes by Injection Locking," *IEEE Photon. Technol. Lett.*, vol. 8, no. 1, pp. 34-36, 1996.
- [5] T. B. Simpson, J. M. Liu, and A. Gavrielides, "Bandwidth Enhancement and Broadband Noise Reduction in Injection-Locked Semiconductor Lasers," *IEEE Photon. Technol. Lett.*, vol. 7, no. 7, pp. 709-711, 1995.
- [6] T. B. Simpson and J. M. Liu, "Enhanced Modulation Bandwidth in Injection-Locked Semiconductor Lasers," *IEEE Photon. Technol. Lett.*, vol. 9, no. 10, pp. 1322-1324, 1997.
- [7] D. J. Malyon, and A. P. McDonna, "102 km Unrepeated Monomode Fibre System Experiment at 140 Mbit/s with an Injection-Locked 1.52  $\mu\text{m}$  Laser Transmitter," *Electron. Lett.*, vol. 18, no. 11, pp. 445-446, 1982.
- [8] H. Toba, Y. Kobayashi, and K. Yanagimoto, "Injection-Locking Technique Applied to a 170 km Transmission Experiment at 445.8 Mbit/s," *Electron. Lett.*, vol. 20, no. 9, pp. 370-371, 1984.
- [9] X. J. Meng, Dennis T. K. Tong, Tai Chau, and Ming C. Wu, "Demonstration of an Analog Fiber-Optic Link Employing a Directly Modulated Semiconductor Laser with External Light Injection," *IEEE Photon. Tech. Lett.*, vol. 10, no. 11, pp. 1620-1622, 1998.
- [10] L. Goldberg, H. F. Taylor, and J. F. Weller, "FM Sideband Injection Locking of Diode Lasers," *Electron. Lett.*, vol. 18, no. 23, pp. 1019-1020, 1982.
- [11] W. I. Way, "Subcarrier Multiplexed Lightwave System Design Considerations For Subscriber Loop Applications," *Journal of Lightwave Technology*, vol. 7, no. 11, pp. 1806-1818, 1989.

- [12] L. Noel, D. Wake, D. G. Moodie, D. D. Marcenac, L. D. Westbrook, and D. Nasset, "Novel Techniques for high-capacity 60-GHz Fiber-Radio Transmission Systems," *IEEE Transactions on microwave theory and techniques*, vol. 45, no. 8, pp. 1416-1423, 1997.
- [13] O. Lidoyne, P. B. Gallion, and D. Erasme, "Modulation Properties of an Injection-Locked Semiconductor Laser," *IEEE J. Quantum Electron.*, vol. QE-27, no.3, 1991.
- [14] J. C. Cartledge and G. S. Burley, "The Effect of Laser Chirping on Lightwave System Performance," *J. Lightwave Technology*, vol. 7, no. 3, pp. 568-573, 1989.
- [15] J. Troger, P.-A. Nicati, L. Thevenaz, and Ph. A. Robert, "Novel Measurement Scheme for Injection-Locking Experiments," *IEEE J. Quantum. Electron.*, vol. 35, no. 1, pp. 32-38, 1999.
- [16] G.Yabre, "Effect of Relatively Strong Light Injection on the Chirp-to-Power Ratio and the 3 dB bandwidth of Directly Modulated semiconductor lasers," *J. Lightwave Technol.*, vol. 14, no. 10, pp2367-2373, 1996.
- [17] G. P. Agrawal and N. K. Dutta, *Semiconductor Laser – 2nd Edition, Van Nostrand Reinhold*, pp. 231-318, 1993.
- [18] C. Lin, and F. Mengel, "Reduction of frequency chirping and dynamic linewidth in high-speed directly modulated semiconductor lasers by injection locking," *Electron. Lett.*, vol. 20, no. 25/26, pp.1073-1075, 1984.
- [19] L. Goldberg, H. F. Taylor, and J. F. Weller, "Microwave signal generation with injection-locked laser diodes," *Electron. Lett.*, vol. 19, no. 13, pp. 491-493, 1983.
- [20] B. Wilson, Z. Ghassemlooy, and I. Darwazeh, *Analogue OPTICAL FIBRE communications, The Institution of Electrical Engineers*, pp. 177-227, 1995.
- [21] L. Goldberg, A. M. Yurek, H. F. Taylor, and J. F. Weller, "35 GHz Microwave Signal Generation with an Injection-Locked Laser Diode," *Electron. Lett.*, vol. 21, no. 18, pp. 814-815, 1985.
- [22] R. W. Tkach and F. Forghieri, "Lightwave System Limitation of Nonlinear Optical Effects," *22nd European Conference on Optical Communication – ECOC'96*, TuB.3.1, 1996.
- [23] P. J. Corvini and T. L. Koch, "Computer Simulation of High-Bit-Rate Optical Fiber Transmission Using Single-Frequency Lasers," *J. Lightwave Tech.*, vol. LT-5, no. 11, pp. 1591-1595, 1987.
- [24] G. Yabre and J. L. Bihan., "Reduction of Nonlinear Distortion in Directly

Modulated Semiconductor Lasers by Coherent Light Injection," *IEEE J. Quantum. Electron.*, vol. 33, no. 7, pp. 1132-1140, 1997.

- [25] R. Lang, "Injection Locking Properties of a Semiconductor Laser," *IEEE J. Quantum. Electron.*, vol. 18, no. 6, pp. 976-983, 1982.
- [26] S. Sivaprakasam, and R. Singh, "Gain change and threshold reduction of diode laser by injection-locking," *Optics Communications*, 151, pp. 253-256, 1998.

Abstract

## **The Characteristics and Applications of the Semiconductor Lasers with Injection Locking**

The characteristics, modulation responses and applications of the semiconductor laser with injection locking have been investigated. For the theoretical analysis, the well-known rate-equations under the external optical injection are used. The locking conditions are obtained through the steady-state solution of the rate-equations. The locking characteristics are distinctively different at different locking conditions.

The small- / large- signal analysis of the equations shows that the optical injection locking (OIL) can not only enhance the modulation bandwidth, but also reduce the frequency chirp significantly. In addition, the reduction of the frequency chirp, related with the laser FM response, results in the improvement of the nonlinear distortion of the laser under multi-tone rf-modulation. In particular, the nonlinearity improvement of the lasers with injection locking under two-tone rf-modulation has been experimentally confirmed.

The influence of the enhanced laser characteristics by OIL with the overall system performance is investigated through the estimation of the bit error rate for a model transmission system. The dependence of the system performance on injected power, transmission length, extinction ratio, and transmission speed is taken into account. It is found that OIL technique can be advantageous for the high-capacity long-span fiber-optic transmission system. Its transmission span is limited only by fiber loss. The experimental implementation of strong optical injection locking will be made in near future in order to prove the transmission performance enhancement.

The nonlinearity improvement of the laser by OIL is examined theoretically as well as experimentally. It is believed due to the enhanced laser characteristics by OIL (i.e, modulation bandwidth enhancement and chirp reduction). It is found that the IMP suppression with OIL will be useful in optical analog transmission systems. And, future works are in progress in order to identify the exact cause for non-linearity reduction with optical injection.

Finally, the new optical mm-wave generation method is proposed, using the intrinsic characteristic of the laser under strong optical injection. In the unstable-locking conditions, the laser generates the multiple optical sidebands separated by the equal frequency. Feeding these sidebands into two slave lasers, it is possible to generate optical  $\mu$ - / mm- waves without using any external RF source. In addition, the frequency separation can be controlled by the adjustment of the injected power.

---

**Key words** : Injection locking, Modulation bandwidth enhancement,  
Chirp reduction, Nonlinearity improvement,  
optical mm-wave generation